ELSEVIER

Chemical Engineering Journal 127 (2007) 157–165

Chemical Engineering Journal

www.elsevier.com/locate/cej

Rapid removal of trace HCHO from indoor air by an air purifier consisting of a continuous concentrator and photocatalytic reactor and its computer simulation

Fumihide Shiraishi [a,*], Takeshi Nomura [b], Shunsuke Yamaguchi [b], Yusuke Ohbuchi [b]

[a] *Department of Bio-System Design, Bio-Architecture Center, Kyushu University, 3-1-1, Maidashi, Higashi-ku, Fukuoka 812-8582, Japan*
[b] *Department of Biochemical Engineering and Science, Faculty of Computer Science and Systems Engineering, Kyushu Institute of Technology, Iizuka 820-8502, Japan*

Received 8 June 2006; received in revised form 1 September 2006; accepted 15 September 2006

Abstract

A mathematical model has been constructed for the removal of gaseous HCHO at a very low concentration level in a closed room by use of an air purifier that consists of a photocatalytic reactor combined with a continuous adsorption and desorption concentrator and the performance of the air purifier has been evaluated by computer simulation. The calculated result for the time course of the HCHO concentration in a 10 m^3 closed room shows that the mathematical model can satisfactorily describe the time-transient behavior of the experimental values. The computer simulation for the treatment of HCHO in an actual dwelling house with the continuous release of HCHO from the building materials indicates that the air purifier can steadily keep the HCHO concentration below the WHO guideline (<80 ppb).

Keywords: Photocatalytic reactor; Continuous concentrator; Mathematical model; Formaldehyde; Computer simulation

1. Introduction

Various photocatalytic methods have been reported on the oxidative decomposition of volatile organic compounds (VOCs) [1–5]. However, the photocatalytic reactions become very slow in the low concentration region of reactants [6–9]. For instance, when the VOC concentrations decrease below 1 parts per million in volume (ppmv), the rates of decomposition of the VOCs are remarkably decreased. This is mainly caused by the film-diffusional resistance significantly increased with decreasing VOC concentration and the insufficient UV light intensity per unit area [10].

We have recently developed a photocatalytic reactor with a parallel array of nine light sources that were fixed in their respective glass tubes [11,12]. As a result of experimental investigation, we found that this reactor can certainly decompose formaldehyde (HCHO) at a concentration level of parts per billion in volume (ppbv) toward a zero concentration because the film-diffusional resistance in the neighborhood of the photocatalyst was completely removed and the UV light intensity per unit surface was sufficiently high. Nevertheless, the performance of the reactor was still insufficient in practical application because the reactor was unable to purify a large amount of air in several hours. To overcome this difficulty, we have developed a new type of air purifier [13], which continuously concentrates harmful chemical substances in the indoor air into a small box by use of a continuous adsorption and desorption concentrator (simply referred to as a continuous concentrator) and then decomposes the concentrated chemical substances by use of the photocatalytic reactor described above. The experimental result for the treatment of trace HCHO in 10 m^3 air showed that the air purifier decreases the HCHO concentration to the neighborhood of the WHO guideline (80 ppbv) in 10 min by the action of the continuous concentrator and then toward a zero concentration by the action of the photocatalytic reactor on the concentrated HCHO. However, the reactor performance under various operational conditions must be further evaluated for the practical application. We consider that the use of the mathematical model is indispensable to achieve this purpose.

In the present work, therefore, we will construct a mathematical model for the treatment of gaseous HCHO with the air

* Corresponding author. Tel.: +92 642 6847; fax: +92 642 6847.
E-mail address: fumishira@brs.kyushu-u.ac.jp (F. Shiraishi).

1385-8947/$ – see front matter © 2006 Elsevier B.V. All rights reserved.
doi:10.1016/j.cej.2006.09.018

Nomenclature

C_B	formaldehyde concentration in a closed room (mg m^{-3})
C_R	formaldehyde concentration on a honeycomb rotor (mg m^{-3})
C_S	formaldehyde concentration in a small box (mg m^{-3})
k	rate constant for a photocatalytic reaction (mg m^{-2} min^{-1})
k_1	rate constant for adsorption of HCHO in a closed room onto a honeycomb rotor (m^3 min^{-1})
k_{-1}	rate constant for desorption of HCHO on a rotor into a closed room (min^{-1})
k_2	rate constant for desorption of HCHO on a rotor into a small box (min^{-1})
k_{-2}	rate constant for adsorption of HCHO in a small box onto a honeycomb rotor (m^3 min^{-1})
k_F	rate constant for release of HCHO from floor in a closed room (mg m^{-2} min^{-1})
k_W	rate constant for release of HCHO from wall and ceiling in a closed room (mg m^{-2} min^{-1})
K_H	adsorption equilibrium constant for a photocatalytic reaction (m^3 mg^{-1})
r_B	rate of adsorption of HCHO in a closed room onto a honeycomb rotor (mg m^{-3} min^{-1})
r_S	rate of desorption of HCHO on a rotor into a small box (mg m^{-3} min^{-1})
S	total surface area of a thin film of titanium oxide on inside surfaces of glass tubes (m^2)
S_F	surface area of floor in a closed room (m^2)
S_R	apparent surface are of a honeycomb rotor (m^2)
S_W	total surface area of wall and ceiling in a closed room (m^2)
t	time (min)
V_B	volume of a closed room (m^3)
V_S	volume of a small box (m^3)

Subscript and superscript

0	initial value
eq	at equilibrium

purifier and elucidate the performance of this apparatus by computer simulation.

2. Experimental

2.1. Materials

Amorphous titanium oxide was synthesized according to the procedure described elsewhere [14–16]. An aqueous solution of 37% formaldehyde was purchased from Wako Pure Chemical Co., Ltd. (Osaka, Japan). Nine Pyrex glass tubes, 28 mm in inside diameter, 210 mm long, and 2 mm in wall thickness, were used as the photocatalyst support. Nine 6-W blacklight blue fluorescent lamps with a wavelength range of 300–390 nm (FL6BL-B; Matsushita Electric Co., Ltd., Tokyo, Japan) were used as the light source [6,17,18].

2.2. Experimental apparatus and method

The photocatalytic reactor with a parallel array of nine UV light sources is shown in Fig. 1. The air containing HCHO was sucked from the bottom of the reactor with the electric fan fixed at the upper part of the reactor and allowed to pass through the annulus of each glass tube. The flow rate of the air was at 11 m s^{-1}, which was sufficient to completely remove the film-diffusional resistance [6]. Since the distance between the internal surface of the glass tube and the external surface of the UV lamp was only 5 mm, the UV intensity per unit surface area was always kept high, which made it possible to decrease a very low concentration of HCHO to a further low concentration. Moreover, since the glass tubes were coated with a transparent thin film of titanium oxide, the UV light that penetrated through the wall of a glass tube contributed to an increase in the rate of reaction [11,19,20].

As shown in Fig. 1, the continuous concentrator consists of a ceramic paper rotor that loaded activated carbon particles of 47.1 kg m^{-3}, two electric fans for adsorption and desorption, and a heater for desorption [11]. The cylindrical rotor has a diameter of 320 mm and thickness of 50 mm; the effective sectional area of the honeycomb laminar with a corrugate pitch of 3 mm is the part bound by circles with diameters of 60 and 300 mm. The total surface area of the honeycomb laminar with a specific surface area of 2955 m^2 m^{-3} was estimated as 10 m^2. The entrance and exit of the desorption part of the continuous concentrator were connected in a loop with the small box of 0.09 m^3 in volume. The air containing HCHO in the closed room was continuously supplied to the adsorption part of the rotor rotating slowly at a constant rate (1 rotation/6 min), so that HCHO was adsorbed on the rotor. The air circulating in the loop was heated with a hot wire just before passing through the desorption part of the rotor and the HCHO adsorbed was desorbed into the loop. Consequently, HCHO in the closed room was continuously concentrated into the loop with the small box.

We designed the concentrator to give a concentration ratio of 10:1 between the small box and closed room. To achieve this, the flow rates of the air that enters the adsorption and desorption parts of the rotor must be set at a ratio of 10:1. Also, the ratio of their sectional areas must be set at the same ratio. Thus, the air in the closed room was supplied to the 5/6 part of the sectional area of the rotor at a flow rate of 2.02 m^3 min^{-1}, while the air heated in the loop was supplied to the 1/12 part of the sectional area of the rotor at a flow rate of 0.220 m^3 min^{-1}. The rest sectional area (1/12 part) was used to preheat the rotor by allowing the air in the loop to pass through the part. The temperature of the desorption air before entering the rotor was set at 180 °C. The HCHO concentrated in the loop was decomposed in the photocatalytic reactor placed in the small box.

All the experiments were performed in a closed room (10 m^3 in volume), made of steel frames covered with polyvinyl chloride

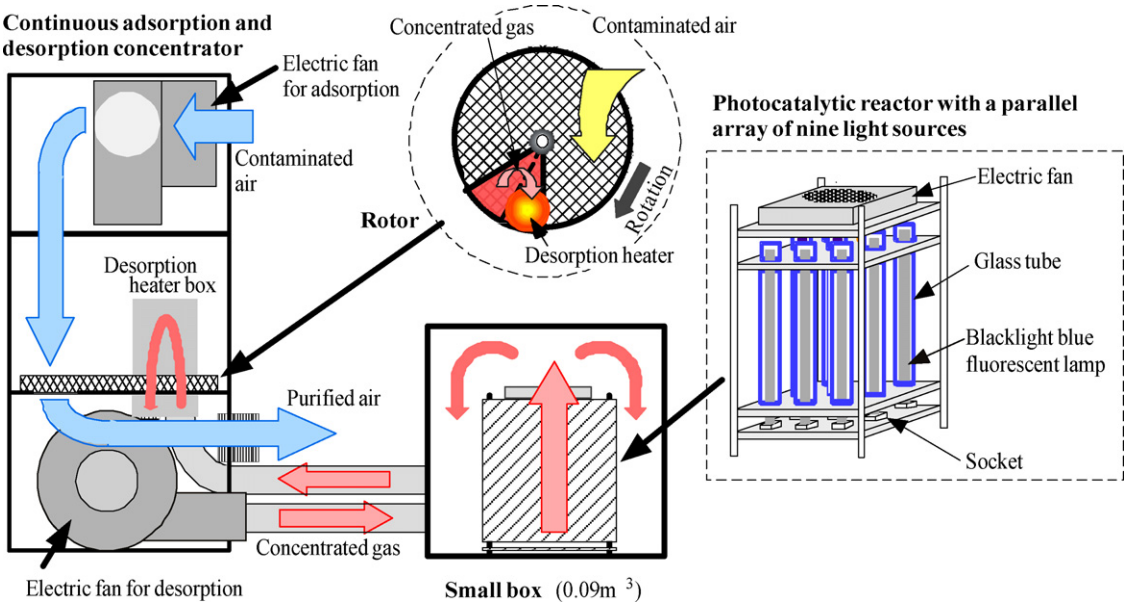

Fig. 1. Schematic of an air purifier that consists of a continuous adsorption and desorption concentrator and photocatalytic reactor.

films. Besides the air purifier, the following instruments were placed in the closed room; a heating plate for instantaneously evaporating HCHO, two electric fans for mixing the air, and a small air pump for periodically sampling the air. The result of a preliminary adsorption experiment indicated that the rate of adsorption of HCHO onto the wall of the closed room was negligibly small compared with that onto the rotor.

The adsorption experiment was performed as follows:

(1) A specified amount of aqueous HCHO solution was put on the heating plate and the room was then closed quickly.
(2) The heating plate was switched-on at once to evaporate HCHO.
(3) The two electric fans were also switched-on to perfectly mix the air.
(4) After 10 min, the air was bubbled through 4.0 ml of distilled water at a flow rate of 0.40 l min^{-1} for 5 min to measure the initial HCHO concentration.
(5) The concentrator was switched-on to start the experiment.
(6) At specified time intervals, the air was bubbled through distilled water to take a sample, as described above.
(7) One milliliter of the sample water was used to measure the HCHO concentration by use of Test Wako for HCHO (Wako Pure Chemical Co., Ltd.). The analytical method is described in detail elsewhere [6].

In the desorption experiment, a specified amount of HCHO was adsorbed in advance onto the rotor. After switching-off the electric fan for adsorption, the electric wire and fan for desorption were switched-on to desorb the adsorbed HCHO into the small box. The following procedure was the same as the procedure (4)–(7) in the adsorption experiment. In the photocatalytic decomposition experiment, the concentrator and photocatalytic reactor were switched-on at the same time to start the experiment.

The HCHO concentration in the small box was measured with gas detector tubes for HCHO (No.91, No91L, and No91LL; GASTEC Co., Ltd., Tokyo, Japan) because the volume of the small box was only 0.09 m^3.

3. Mathematical models

3.1. Model for adsorption of HCHO on an activated carbon rotor

We assume that there is the following equilibrium relationship between the gaseous HCHO in the closed room, referred to as B, and the HCHO adsorbed on the rotor with a total surface area (S_R) of 10 m^2, referred to as R.

$$\underset{10\,\mathrm{m^3\ room}}{\mathrm{B}} \underset{k_{-1}}{\overset{k_1}{\rightleftarrows}} \underset{\mathrm{Rotor}}{\mathrm{R}}$$

Since the HCHO concentration is usually on the order of ppb, the rates of adsorption and desorption are assumed to follow first-order kinetics. As a result, the time course of the HCHO concentration in the closed room with a volume of V_B (=10 m^3), i.e., C_B, is written as

$$V_B \frac{dC_B}{dt} = -k_1 C_B + k_{-1} S_R C_R. \quad (1)$$

We now consider a case where the HCHO uniformly distributed in the air in the closed room is adsorbed onto the rotor and there is no HCHO adsorbed on the rotor at the starting time. If the operation of the desorption is carried out, Eq. (1) gives the following relationship between the initial rate of adsorption r_{B0} and the initial HCHO concentration C_{B0}.

$$r_{B0} = -\left.\frac{dC_B}{dt}\right|_{t=0} = \frac{1}{V_B} k_1 C_{B0} \quad (2)$$

If the r_{B0} values measured are plotted against the C_{B0} values, the slope of the straight line drawn on the plot gives the rate constant for adsorption k_1. Under an equilibrium condition, moreover, Eq. (1) gives

$$k_{-1} = k_1 \frac{C_B^{eq}}{V_B(C_{B0} - C_B^{eq})}. \quad (3)$$

Application of the HCHO concentrations at equilibrium in the closed room and on the rotor and the k_1 value determined above to Eq. (3) provides the rate constant for desorption k_{-1}.

3.2. Model for desorption of HCHO from an activated carbon rotor

We consider a mathematical model for the case where the HCHO adsorbed on the rotor is desorbed into the small box with a volume of V_S (=0.09 m^3). When a known amount of HCHO is adsorbed on the rotor in advance and then desorbed by passing the heated air thorough a part of the rotor, we assume the following equilibrium relationship between the HCHO on the rotor and the gaseous HCHO in the small box:

$$\underset{\text{Rotor}}{\text{R}} \underset{k_{-2}}{\overset{k_2}{\rightleftarrows}} \underset{\text{Small box}}{\text{S}}$$

When expressing the HCHO concentration on the rotor as C_R and the gaseous HCHO concentration in the small box as C_S, the time course of C_S is written as

$$V_S \frac{dC_S}{dt} = k_2 S_R C_R - k_{-2} C_S. \quad (4)$$

Under the assumption that there does not exist HCHO in the air in the small box at the starting time, the relationship between the initial rate of desorption of gaseous HCHO in the small box r_{S0} and the initial HCHO concentration on the rotor C_{R0} is given as

$$r_{S0} = \left.\frac{dC_S}{dt}\right|_{t=0} = \frac{S_R}{V_S} k_2 C_{R0}. \quad (5)$$

A linear plot of r_{S0} against C_{R0} gives the rate constant for desorption k_2 from its slope. Also, under an equilibrium condition, Eq. (4) gives

$$k_{-2} = k_2 \frac{S_R C_{R0} - V_S C_S^{eq}}{C_S^{eq}}. \quad (6)$$

Therefore, application of the HCHO concentrations in the small box and on the rotor at equilibrium and the k_2 value determined above gives the rate constant for adsorption k_{-2}.

3.3. Model for continuous adsorption and desorption of HCHO

When simultaneously performing the adsorption of HCHO in the closed room onto the honeycomb rotor and the desorption of the adsorbed HCHO into the small box by use of the continuous concentrator, we express these relationships as follows:

$$\underset{10\,\text{m}^3\ \text{room}}{\text{B}} \underset{k_{-1}}{\overset{k_1}{\rightleftarrows}} \underset{\text{Rotor}}{\text{R}} \underset{k_{-2}}{\overset{k_2}{\rightleftarrows}} \underset{\text{Small box}}{\text{S}}$$

The concentration of HCHO adsorbed on the surface of the adsorption part is not uniform during the adsorption and desorption operation. To avoid the complication of the mathematical model, however, the average value of the concentration of HCHO adsorbed over the entire surface of the adsorption part of the rotor is chosen for C_R. The differential equations for the HCHO concentrations in the closed room, on the rotor, and in the small box are written as follows:

$$V_B \frac{dC_B}{dt} = -k_1 C_B + k_{-1} S_R C_R \quad (7)$$

$$S_R \frac{dC_R}{dt} = k_1 C_B - k_{-1} S_R C_R - k_2 S_R C_R + k_{-2} C_S \quad (8)$$

$$V_S \frac{dC_S}{dt} = k_2 S_R C_R - k_{-2} C_S \quad (9)$$

3.4. Model for simultaneous operation of continuous adsorption and desorption and photocatalytic decomposition of HCHO

When simultaneously performing the adsorption of HCHO in the closed room onto the honeycomb rotor, the desorption of the adsorbed HCHO into the small box, and the photocatalytic decomposition of the desorbed HCHO in the small box, we express these relationships as follows:

$$\underset{10\,\text{m}^3\ \text{room}}{\text{B}} \underset{k_{-1}}{\overset{k_1}{\rightleftarrows}} \underset{\text{Rotor}}{\text{R}} \underset{k_{-2}}{\overset{k_2}{\rightleftarrows}} \underset{\text{Small box}}{\text{S}} \xrightarrow{k, K_H} \underset{\text{Products}}{\text{T}}$$

The differential equations for the HCHO concentrations at the three places can be written as follows:

$$V_B \frac{dC_B}{dt} = -k_1 C_B + k_{-1} S_R C_R \quad (10)$$

$$S_R \frac{dC_R}{dt} = k_1 C_B - k_{-1} S_R C_R - k_2 S_R C_R + k_{-2} C_S \quad (11)$$

$$V_S \frac{dC_S}{dt} = k_2 S_R C_R - k_{-2} C_S - \frac{S k K_H C_S}{1 + K_H C_S} \quad (12)$$

As previously reported, the photocatalytic decomposition of HCHO follows Langmuir–Hinshelwood type kinetics. We use the values of 0.458 mg m^{-2} min^{-1} and 0.654 m^3 mg^{-1} previously determined for the rate constant for reaction k and the adsorption equilibrium constant K_H, respectively [21]. The total surface area of the photocatalyst on the inside surfaces of nine glass tubes, S, is 0.182 m^2.

3.5. Model for continuous concentration and photocatalytic decomposition of HCHO under steady release of HCHO from room materials

When treating the air that contains HCHO by the continuous concentrator and photocatalytic reactor under the steady

Table 1
Sizes of rooms set up for simulation (Chukyo-size room)

Size [mat]	Area of floor [m^2]	Total area of wall and ceiling [m^2]	Volume [m^3]
6	9.92	37.2	24.3
8	13.2	40.5	33.0
12	19.8	56.2	37.2

release of HCHO from the wall, ceiling, and floor of the room, we express these relationships as follows:

$$\underset{\text{Wall, floor, ceiling}}{\text{W}} \xrightarrow{k_F, k_W} \underset{10\,\text{m}^3\text{ room}}{\text{B}} \underset{k_{-1}}{\overset{k_1}{\rightleftarrows}} \underset{\text{Rotor}}{\text{R}} \underset{k_{-2}}{\overset{k_2}{\rightleftarrows}} \underset{\text{Small box}}{\text{S}} \xrightarrow{k, K_H} \underset{\text{Products}}{\text{T}}$$

The differential equations for the HCHO concentrations at their respective places can be written as follows:

$$V_B \frac{dC_B}{dt} = -k_1 C_B + k_{-1} S_R C_R + k_F S_F + k_W S_W \quad (13)$$

$$S_R \frac{dC_R}{dt} = k_1 C_B - k_{-1} S_R C_R - k_2 S_R C_R + k_{-2} C_S \quad (14)$$

$$V_S \frac{dC_S}{dt} = k_2 S_R C_R - k_{-2} C_S - \frac{S k K_H C_S}{1 + K_H C_S} \quad (15)$$

The surface areas of the wall, floor, and ceiling and the amounts of the air for the rooms of 6, 8, and 12 tatami mats are given in Table 1, where we assumed that the rooms are in a Chukyo-size room (1.81 m × 0.91 m for one mat) in width and 2.5 m in height. The rate constants for the steady release of HCHO from the floor k_F and for that from both the wall and ceiling k_W have been reported to be 4.67×10^{-5} mg m^{-2} min^{-1} and 6.33×10^{-5} mg m^{-2} min^{-1}, respectively [22]. All the differential equations were numerically solved by Runge–Kutta method.

4. Results and discussion

4.1. Adsorption experiment

Aqueous solutions of HCHO at various concentrations were volatilized in the closed room and adsorption experiment of HCHO onto the rotor was performed by rotating the electric fan for adsorption. The time courses of the HCHO concentrations in the closed room are shown in Fig. 2. The HCHO concentration initially decreases quickly and then stops decreasing, probably because the desorption of HCHO from the rotor into the closed room proceeds with the adsorption of HCHO onto the rotor and these two processes finally reach equilibrium.

The initial rates of adsorption, determined from the experimental data in Fig. 2, are plotted against their respective initial concentrations of HCHO in Fig. 3. There is a linear relationship between them. The desorption of HCHO from the rotor is negligible in the initial stage of the adsorption. Therefore, we applied Eq. (2) to the experimental data in Fig. 3 and determined the expression of the best fitting straight line by the least-square method. From the slope of the straight line, the rate constant for adsorption k_1 was determined to be 1.79 m^3 min^{-1}. Under

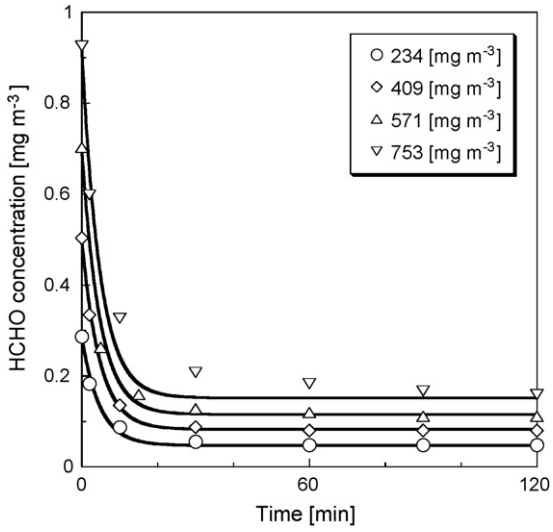

Fig. 2. Time courses of HCHO concentrations in a 10 m^3 closed room by adsorption operation.

the assumption of equilibrium, we also determined k_{-1} to be 0.0349 min^{-1} from Eq. (3).

The rate constants thus determined were applied to Eq. (1), which was solved numerically by the Runge–Kutta method to obtain the time course of the HCHO concentration. The calculated results, shown by solid lines in Fig. 2, are in satisfactory agreements with the experimental values.

4.2. Desorption experiment

After the adsorption experiment, the rotor slowly rotating was heated by supplying the heated air to desorb the adsorbed HCHO into the closed room. The time courses of the gaseous HCHO concentrations in the closed room are shown in Fig. 4. It is clear that the HCHO concentration stops decreasing before the complete desorption of HCHO. The percentage of desorption (a ratio

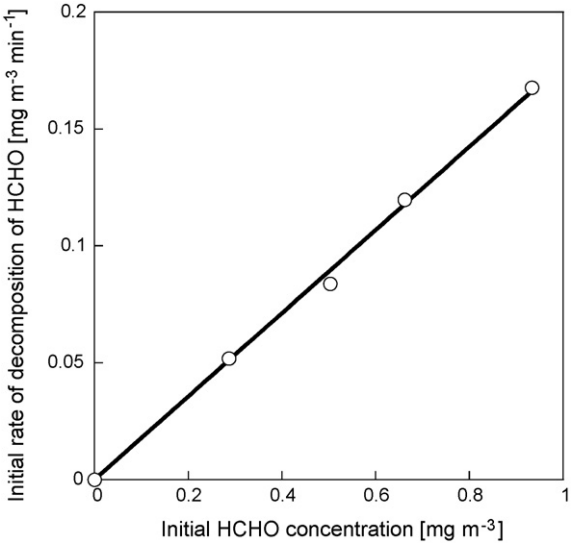

Fig. 3. Relationship between initial rate of decomposition of HCHO and initial HCHO concentration.

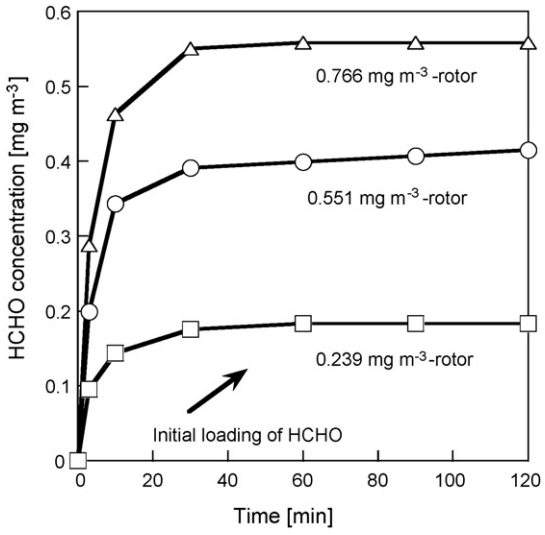

Fig. 4. Time courses of HCHO concentrations in a 10 m^3 closed room by desorption operation.

of HCHO desorbed from the rotor to HCHO initially absorbed on the rotor) was about 75%. Fig. 5 shows a plot of the initial rate of desorption of HCHO determined from the experimental values in Fig. 4 against the concentration of HCHO initially absorbed on the rotor. It is clear that there is a linear relationship between these experimental variables.

The entrance and exit of the continuous concentrator were connected in a loop with the small box and the desorption experiment of the HCHO adsorbed on the rotor was performed as in the previous section. The time courses of the HCHO concentrations in the small box, thus determined, are shown in Fig. 6. The HCHO concentrations reach their respective maximums after 5 min and then decrease slowly, which is probably due to the gradual leakage of HCHO from the side wall of the small box into the closed room. This problem can be solved by improving the small box. From the maximum value of the HCHO concentration when the amount of HCHO adsorbed on the rotor is 5.99 mg m^{-3}, moreover, it is clear that HCHO is concentrated up to about 10-fold, compared with the experimental values for almost the same initial loading of HCHO in Fig. 4. It is considered that the about 10-fold increase in the percentage of concentration, despite the volume ratio of 111 times between the closed and small rooms, is based on the equilibrium relationship between the HCHO concentrations on the rotor and in the small box. From the increased ratio of concentration, nevertheless, it is evident that HCHO can be decomposed in shorter time.

The adsorption of HCHO in the small box onto the rotor can be neglected in the initial stage of the desorption. Therefore, we applied Eq. (5) to the experimental values plotted in Fig. 5 in order to determine the expression of the best-fitting straight line, the slope of which gave the rate constant for desorption as $k_2 = 0.0609\ \mathrm{min}^{-1}$. Moreover, we assumed in Fig. 6 that the system reached equilibrium after the HCHO concentrations in the small box took their respective maximums and then determined k_{-2} to be $0.0885\ \mathrm{m}^3\ \mathrm{min}^{-1}$ from Eq. (6).

The rate constants thus obtained were applied to Eq. (4), which was then solved by the Runge–Kutta method to obtain the time course of the HCHO concentration in the desorption of HCHO into the small box. The calculated results are shown by solid lines in Fig. 6, indicating that HCHO is desorbed promptly from the rotor into the small box and reaches its equilibrium concentration.

4.3. Continuous concentration experiment by adsorption and desorption of HCHO

The HCHO in the closed room was adsorbed onto the rotor while the HCHO adsorbed was desorbed into the small box by use of the continuous concentrator. The experimental result is shown in Fig. 7, where the solid line shows the calculated result; all the rate constants determined were applied to Eqs. (7)–(9) to solve the differential equations by the Runge–Kutta method. The calculated results are in satisfactory agreements with both the

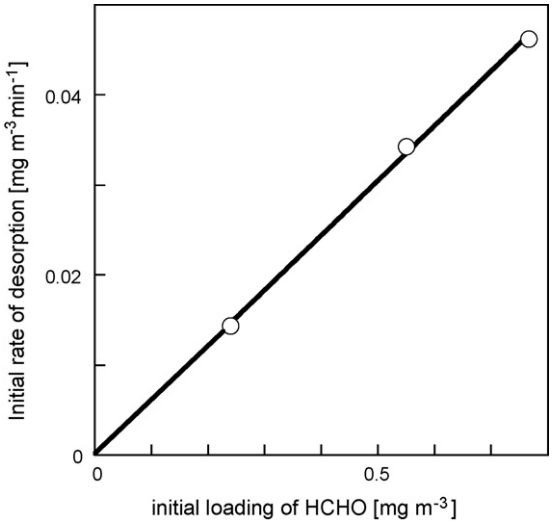

Fig. 5. Relationship between initial rate of desorption of HCHO from a rotor and initial amount of HCHO adsorbed on a honeycomb rotor loading activated carbon particles.

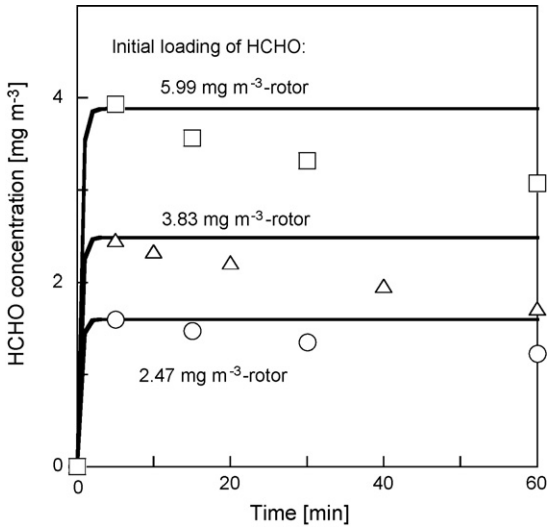

Fig. 6. Time courses of HCHO concentrations in a 0.09 m^3 small box by desorption operation.

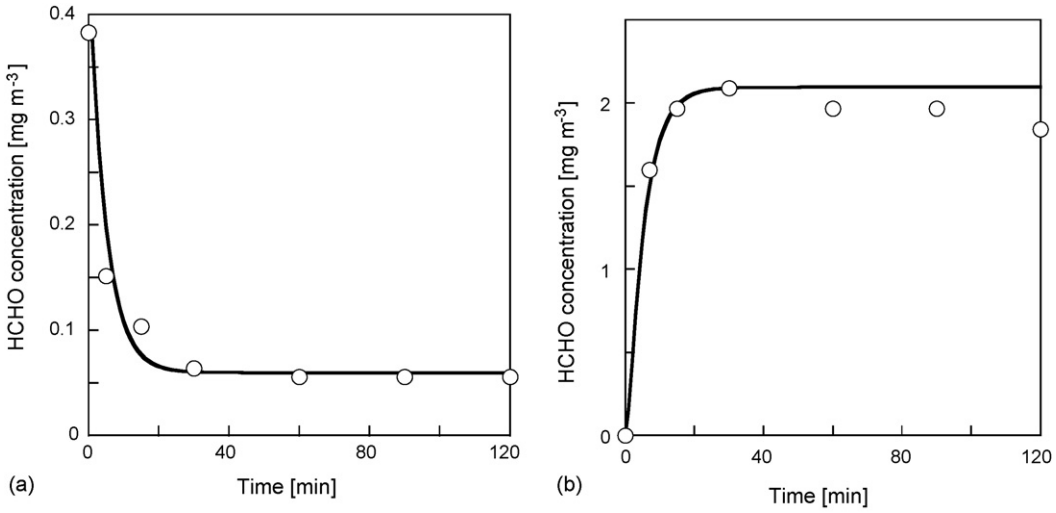

Fig. 7. Time courses of HCHO concentrations in (a) a 10 m^3 closed room and (b) a 0.09 m^3 small box in treatment of air by use of a continuous concentrator without operation of a photocatalytic reactor.

experimental values for the closed room and small box. Also, the facts that the initial concentration of HCHO in the closed room is 0.38 mg m^{-3} and the equilibrium concentration of HCHO in the small box reaches 2 mg m^{-3} indicate that the concentration of about five-fold was attained, which obviously contributes to an increase in the rate of the photocatalytic reaction. It is also clear that when HCHO in the closed room is removed with only the continuous concentrator, the increase in the HCHO concentration stops at the concentration in the neighborhood of the WHO guideline (0.09 mg m^{-3}), owing to reaching equilibrium between the HCHO concentrations in the closed room and on the rotor and between those on the rotor and in the small box.

4.4. Removal of HCHO by simultaneous use of a continuous concentrator and photocatalytic reactor

HCHO in the closed room was concentrated into the small box by use of the continuous concentrator and, at the same time, the HCHO concentrated was decomposed by use of the photocatalytic reactor in the small box. The time courses of the HCHO concentrations are shown in Fig. 8. For comparison, the experimental values for the decomposition of HCHO in the photocatalytic reactor directly placed in the closed room are also plotted in this figure. In the case of the photocatalytic reactor alone, the HCHO concentration decreases almost linearly, but it takes more than one day to reach the WHO guideline, which is not practical rate of decomposition. In the simultaneous use of the photocatalytic reactor with the continuous concentrator, on the other hand, the HCHO concentration decreases rapidly toward a zero concentration. The HCHO concentration in the small box takes a maximum value 5 min after the operation and then decreases rapidly. From a comparison of this result with the experimental result in the absence of the photocatalytic reactor, shown in Fig. 7, it is clear that this decrease is due to the fact that HCHO was photocatalytically decomposed in the small box.

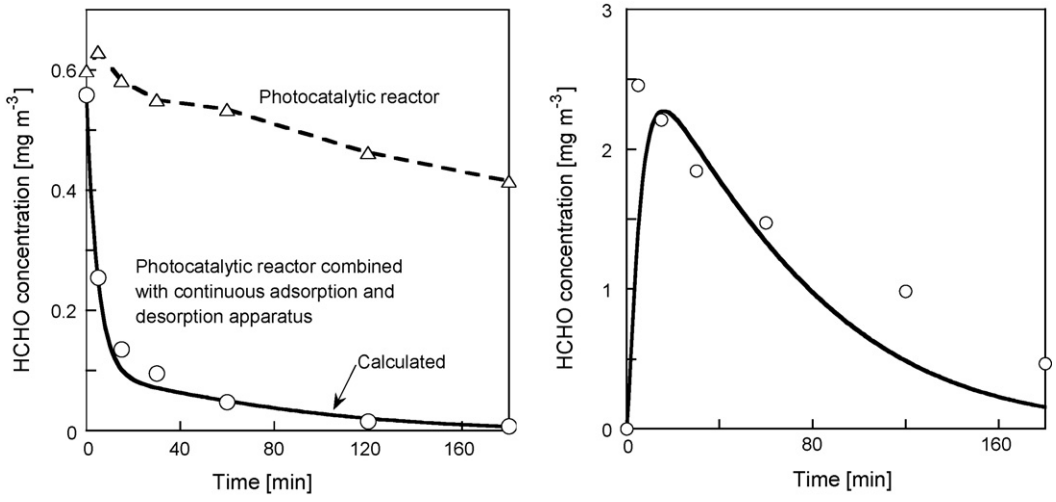

Fig. 8. Time courses of HCHO concentrations in a 10 m^3 closed room and 0.09 m^3 small box in treatment of air by use of an air purifier under operating an photocatalytic reactor and by use of a photocatalytic reactor alone.

All the rate constants determined were applied to Eqs. (10)–(12), which were then solved numerically to calculate the time courses of the HCHO concentrations. The calculated results are shown by solid lines in Fig. 8. One of the purposes of the present work is to construct a mathematical model that can express complicated phenomena for the air purifier reasonably but as simply as possible. As a result, the mathematical model thus obtained may have a limitation to minute description. Nevertheless, the simplified mathematical model accurately expresses the time course of the HCHO concentration in the closed room. It also successfully expresses the time-transient behavior of the HCHO concentration in the small box. Thus, we consider that the mathematical model is sufficient to describe the performance of the air purifier.

4.5. Simulation of treatment of HCHO in an actual dwelling house with continuous release of HCHO from building materials

In an actual dwelling house, HCHO is gradually released from the wall, floor, and ceiling of the room. Therefore, it is necessary to take into consideration the continuous release of HCHO in the mathematical model in order to correctly evaluate the performance of the air purifier. In the following, we will perform computer simulation for the treatment of the indoor air with the air purifier under several conditions where HCHO is continuously released from the building materials into the air in the rooms of 6, 8, and 12 tatami mats.

Fig. 9 shows the changes in the indoor concentrations of gaseous HCHO released from the building materials of the three rooms in the case without HCHO in the closed room at $t = 0$. It should be noted that the rate of increase of the HCHO concentration is not proportional to the increased number of mats because the total surface area of the wall, ceiling, and floor in the three rooms is not exactly proportional to their respective space volumes. In any case, it is certain that the HCHO concentration in the closed room is increased up to the vicinity of the WHO guideline after about 1000 min (16.7 h) as a result of continuous release of HCHO from the building materials.

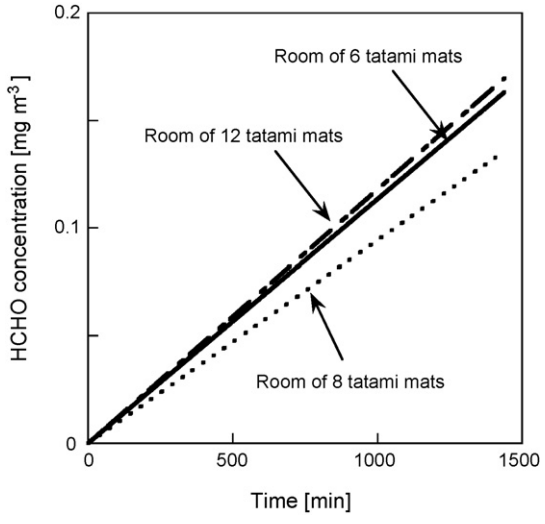

Fig. 9. Simulation for continuous release of HCHO from ceiling, wall, and floor in Chukyo-size rooms of 6, 8, and 12 tatami mats.

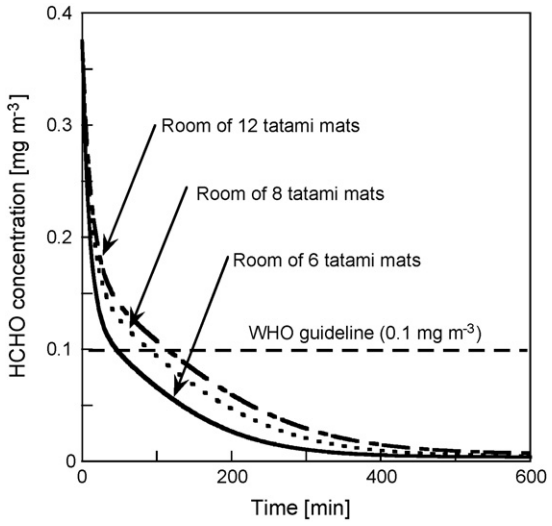

Fig. 10. Simulation for treatment of air in Chukyo-size rooms of 6, 8, and 12 tatami mats under continuous release of HCHO from building materials by use of an air purifier.

Fig. 10 shows the time courses of the HCHO concentration in the three rooms under continuous release of HCHO from the building materials in the treatment of the air with the air purifier. In this simulation, the initial HCHO concentration was assumed to be a value of 0.375 mg m^{-3}, which is close to the HCHO concentration detected in newly built dwelling houses [23]. The calculated results clearly show that the HCHO concentration is quickly decreased below the WHO guideline in 2 h even under the continuous release of HCHO. In this simulation, we assumed that the release of HCHO occurs from the whole surface area of the wall, floor, and ceiling. In the dwelling houses, however, the rate of release of HCHO is considered smaller because of the presence of windows and, therefore, the rate of treatment should be faster.

Since the HCHO adsorbed onto the rotor can be desorbed by supplying the air heated at 120–180 °C, the energy required for heating can be adjusted if necessary. On the other hand, Fig. 9 indicates that it takes 16.7 h until the indoor concentration of HCHO increases from a zero concentration to the WHO guideline. Therefore, one may consider the periodic operation of the air purifier, in which both the concentrator and photocatalytic reactor are initially switched-on until the HCHO concentration is decreased to the neighborhood of a zero concentration and then the photocatalytic decomposition alone is operated in the state of the concentrator switched-off until the HCHO concentration in the closed room is increased to the neighborhood of the WHO guideline. We thus simulated the periodic operation where both the continuous concentrator and photocatalytic reactor are operated until 400 min where the HCHO concentration is reduced to 0.0125 mg m^{-3}, and thereafter, the switching-off and -on of the concentrator are repeated every 5 and 2 h, respectively. The result of simulation shown in Fig. 11 indicates that the periodic operation makes it possible to keep the HCHO concentration less than 0.05 mg m^{-3}.

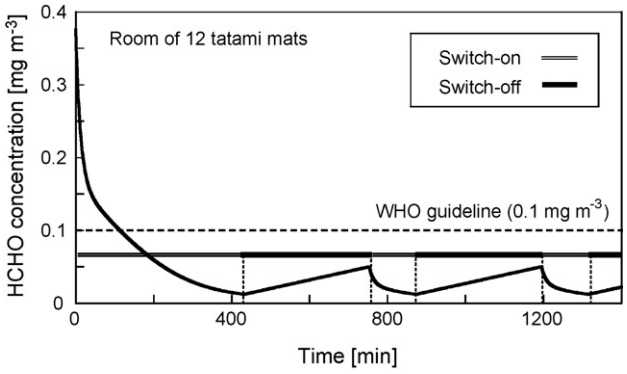

Fig. 11. Time course of HCHO concentration for treatment of air in a Chukyo-size room of 12 tatami mats under continuous release of HCHO from building materials by use of an air purifier.

5. Conclusion

In the present work, we constructed a mathematical model for the removal of gaseous HCHO at a very low concentration level in a closed room by use of an air purifier that consists of a photocatalytic reactor and continuous concentrator. The model calculations were performed for the time courses of the HCHO concentrations in a 10 m^3 closed room and 0.09 m^3 small box. As a result, we found satisfactory agreements of the calculated results with the experimental values. The computer simulation for the treatment of HCHO in an actual dwelling house with the continuous release of HCHO from building materials indicated that the air purifier can steadily keep the gaseous HCHO concentration in a spacious room below the WHO guideline.

References

[1] A.J. Jaira, W.N. Lau, C.Y. Lee, P.L. Yue, C.K. Chan, K.L. Yeung, Performance of a membrane-catalyst for photocatalytic oxidation of volatile organic compounds, Chem. Eng. Sci. 58 (2003) 959–962.

[2] B.-Y. Lee, S.-H. Park, S.-C. Lee, M. Kang, S.-J. Choung, Decomposition of benzene by using a discharge plasma–photocatalyst hybrid system, Catal. Today 93–95 (2004) 769–776.

[3] T. Sano, N. Negishi, K. Takeuchi, S. Matsuzawa, Degradation of toluene and acetaldehyde with Pt-loaded TiO_2 catalyst and parabolic trough concentrator, Solar Energy 77 (2004) 543–552.

[4] J. Zhao, X. Yang, Photocatalytic oxidation for indoor air purification: a literature review, Build. Environ. 38 (2003) 645–654.

[5] S.B. Kim, S.C. Hong, Kinetic study for photocatalytic degradation of volatile organic compounds in air using thin film TiO_2 photocatalyst, Appl. Catal. B: Environ. 35 (2002) 305–315.

[6] F. Shiraishi, D. Ohkubo, K. Toyoda, S. Yamaguchi, Decomposition of gaseous formaldehyde in a photocatalytic reactor with a parallel array of light sources: 1. Fundamental experiment for reactor design, Chem. Eng. J. 114 (2005) 153–159.

[7] S. Wang, F. Shiraishi, K. Nakano, A synergistic effect of photocatalysis and ozonation on decomposition of formic acid in an aqueous solution, Chem. Eng. J. 87 (2002) 261–271.

[8] F. Shiraishi, C. Kawanishi, An effect of diffusional film on formation of hydrogen peroxide in photocatalytic reactions, J. Phys. Chem. A 108 (2004) 10491–10496.

[9] F. Shiraishi, M. Nagano, S. Wang, Characterization of a photocatalytic reaction in a continuous-flow recirculation reactor system, J. Chem. Technol. Biotechnol. 81 (2006) 1039–1048.

[10] J.-H. Xu, F. Shiraishi, Photocatalytic decomposition of acetaldehyde in air over titanium dioxide, J. Chem. Technol. Biotechnol. 74 (1999) 1096–1100.

[11] F. Shiraishi, K. Toyoda, H. Miyakawa, Decomposition of gaseous formaldehyde in a photocatalytic reactor with a parallel array of light sources: 2. Reactor performance, Chem. Eng. J. 114 (2005) 145–151.

[12] F. Shiraishi, Y. Ohbuchi, S. Yamaguchi, K. Yamada, H. Yamauchi, H. Okano, A rapid treatment of indoor formaldehyde at a very low concentration in a photocatalytic reactor system combined with a continuous adsorption and desorption technique, in: Proceedings of the 3rd Eur. Chem. Eng. Cong., Nürnberg, 2001.

[13] F. Shiraishi, S. Yamaguchi, Y. Ohbuchi, A rapid treatment of formaldehyde in a highly-tight room using a photocatalytic reactor combined with a continuous adsorption and desorption apparatus, Chem. Eng. Sci. 58 (2003) 929–934.

[14] F. Shiraishi, T. Nakasako, Z. Hua, Formation of hydrogen peroxide in photocatalytic reactions, J. Phys. Chem. A 107 (2003) 11072–11081.

[15] K. Matsuo, T. Takeshita, K. Nakano, Formation of thin films by the treatment of amorphous titania with H_2O_2, J. Cryst. Growth 99 (1990) 621–624.

[16] S. Jin, F. Shiraishi, Enhanced photocatalytic decompositions of organic compounds over metal-photodepositing titanium dioxide, Chem. Eng. J. 97 (2004) 203–211.

[17] S. Fukinbara, F. Shiraishi, K. Nakano, Characteristics of the photocatalytic reactor with an annular array of glass tubes surrounding a light source: 1. Selection of a light source and photocatalyst support, CELSS J. 13 (2001) 1–10.

[18] S. Fukinbara, F. Shiraishi, Characteristics of the photocatalytic reactor with an annular array of glass tubes surrounding a light source: 2. Kinetic analysis, CELSS J. 13 (2001) 11–23.

[19] S. Wang, F. Shiraishi, K. Nakano, Decomposition of formic acid in a photocatalytic reactor with a parallel array of four light sources, J. Chem. Technol. Biotechnol. 77 (2002) 805–810.

[20] S. Wang, F. Shiraishi, Decomposition of formic acid in two types of photocatalytic reactors: effects of film-diffusional resistance and penetration of UV light on decomposition rates, Eco-Engineering 14 (2002) 9–17.

[21] S. Yamaguchi, Oxidative decomposition of formaldehyde in a photocatalytic reactor and its kinetic analysis, Master's Thesis, Kyushu Institute of Technology, 2000.

[22] T. Nomura, Air purification based on the photocatalytic reaction combined with continuous adsorption and desorption, Master's Thesis, Kyushu Institute of Technology, 2004.

[23] M. Hori, J. Yang, Considerations of volatile organic compounds pollution in dwellings and its measurement and evaluation, J. Human Living Environ. 4 (1996) 61–69.